NASA/TM—2010-216080

Test Method Variability in Slow Crack Growth Properties of Sealing Glasses

J.A. Salem
Glenn Research Center, Cleveland, Ohio

R. Tandon
Sandia National Laboratories, Albuquerque, New Mexico

January 2010

NASA STI Program . . . in Profile

Since its founding, NASA has been dedicated to the advancement of aeronautics and space science. The NASA Scientific and Technical Information (STI) program plays a key part in helping NASA maintain this important role.

The NASA STI Program operates under the auspices of the Agency Chief Information Officer. It collects, organizes, provides for archiving, and disseminates NASA's STI. The NASA STI program provides access to the NASA Aeronautics and Space Database and its public interface, the NASA Technical Reports Server, thus providing one of the largest collections of aeronautical and space science STI in the world. Results are published in both non-NASA channels and by NASA in the NASA STI Report Series, which includes the following report types:

- TECHNICAL PUBLICATION. Reports of completed research or a major significant phase of research that present the results of NASA programs and include extensive data or theoretical analysis. Includes compilations of significant scientific and technical data and information deemed to be of continuing reference value. NASA counterpart of peer-reviewed formal professional papers but has less stringent limitations on manuscript length and extent of graphic presentations.

- TECHNICAL MEMORANDUM. Scientific and technical findings that are preliminary or of specialized interest, e.g., quick release reports, working papers, and bibliographies that contain minimal annotation. Does not contain extensive analysis.

- CONTRACTOR REPORT. Scientific and technical findings by NASA-sponsored contractors and grantees.

- CONFERENCE PUBLICATION. Collected papers from scientific and technical conferences, symposia, seminars, or other meetings sponsored or cosponsored by NASA.

- SPECIAL PUBLICATION. Scientific, technical, or historical information from NASA programs, projects, and missions, often concerned with subjects having substantial public interest.

- TECHNICAL TRANSLATION. English-language translations of foreign scientific and technical material pertinent to NASA's mission.

Specialized services also include creating custom thesauri, building customized databases, organizing and publishing research results.

For more information about the NASA STI program, see the following:

- Access the NASA STI program home page at *http://www.sti.nasa.gov*

- E-mail your question via the Internet to *help@sti.nasa.gov*

- Fax your question to the NASA STI Help Desk at 443–757–5803

- Telephone the NASA STI Help Desk at 443–757–5802

- Write to:
  NASA Center for AeroSpace Information (CASI)
  7115 Standard Drive
  Hanover, MD 21076–1320

NASA/TM—2010-216080

Test Method Variability in Slow Crack Growth Properties of Sealing Glasses

J.A. Salem
Glenn Research Center, Cleveland, Ohio

R. Tandon
Sandia National Laboratories, Albuquerque, New Mexico

Prepared for the
Materials Science and Technology 2008 Conference and Exhibition (MS&T)
sponsored by the ACS, AIST, ASM, and TMS
Pittsburgh, Pennsylvania, October 5–9, 2008

National Aeronautics and
Space Administration

Glenn Research Center
Cleveland, Ohio 44135

January 2010

Acknowledgments

The authors thank J. Jill Glass of Sandia National Laboratories for many useful discussions, and Frank Kody and Sara Caruso of the NASA Summer Intern Program for running the soda-lime silicate SCG tests.

Level of Review: This material has been technically reviewed by technical management.

Available from

NASA Center for Aerospace Information
7115 Standard Drive
Hanover, MD 21076–1320

National Technical Information Service
5285 Port Royal Road
Springfield, VA 22161

Available electronically at http://gltrs.grc.nasa.gov

Test Method Variability in Slow Crack Growth Properties of Sealing Glasses

J.A. Salem
National Aeronautics and Space Administration
Glenn Research Center
Cleveland, Ohio 44135

R. Tandon
Sandia National Laboratories
Albuquerque, New Mexico 87123

Abstract

The crack growth properties of several sealing glasses were measured by using constant stress rate testing in ~2 and 95 percent RH (relative humidity). Crack growth parameters measured in high humidity are systematically smaller (n and B) than those measured in low humidity, and crack velocities for dry environments are ~100x lower than for wet environments. The crack velocity is very sensitive to small changes in RH at low RH. Biaxial and uniaxial stress states produced similar parameters. Confidence intervals on crack growth parameters that were estimated from propagation of errors solutions were comparable to those from Monte Carlo simulation. Use of scratch-like and indentation flaws produced similar crack growth parameters when residual stresses were considered.

Introduction

Sealing glasses are used in components such as electrical feed through connectors. The glass electrically insulates and seals the connector, and thus fracture of the brittle seal is a concern. In applications such as the Space Shuttle Environmental Cut Off (ECO) system, the connector seals are subjected to differential pressures at cryogenic temperatures and seal failure can create leakage of dangerous liquids and/or gasses. Failure can occur even under constant load conditions due to stress corrosion cracking in water vapor.

The slow crack growth parameters of several sealing glasses were measured to compare glasses and to help perform life prediction and reliability analysis of components such as feed through connectors. Strength based measurements, which are convenient, were used to generate the data. However, because the statistical scatter in parameters derived from strength data can be very large, the statistical significance of the estimates was checked by estimation of confidence intervals on the parameters via propagation of errors (POE) and Monte Carlo methods. The large scatter is a result of strength not being a material property for glasses, but a function of the fracture toughness and worst flaw present from a variety of sources. Ideally, parameter estimation and design of brittle materials should be done on a fracture mechanics basis (e.g., NASGRO (Ref. 1)) rather than a strength basis because strength is a function of the highly variable flaw size and relatively consistent fracture toughness.

Although fracture mechanics specimens with large cracks, such as the double-torsion specimen, can be used to measure crack growth with less scatter, the results are complicated by R-curve effects in coarse grain materials such as ZnSe (Ref. 2) and diffusion rate effects when the crack size is large relative to that in real components. Strength based testing can be made more akin to fracture mechanics methods by placing a small precrack, such as an indentation, in specimens and thereby reduce scatter, yet test cracks on the order of those encountered in applications. This work investigates and compares the use of natural flaws and small precracks in strength specimens for the generation of crack growth parameters of glasses. Comparison of parameters from strength methods to those from macro-crack fracture mechanics methods is left to future study.

In order to cover the range of environments to which components with sealing glasses are exposed, RH (relative humidity) of ~2 and 95 percent were considered. To expedite the work, constant stress rate testing of flexure specimens was used. The data was analyzed by linear regression of (1) the individual data points, (2) the median values, and (3) the average values.

In order to investigate the effect of crack type and stress state on parameter variance, an additional set of tests was conducted on a barium-strontium–doped glass by subjecting abraded and indented test specimens to uniaxial and biaxial loading. These flaw types and stress states represent the flaws and loads that lead to failure in real components, and could be produced when a hard tool impacts the surface directly or at a shallow angle.

Materials

The sealing glasses tested[1] were Corning 0120, Electro-Glass 2164, Schott 8330 borosilicate glass, and Schott S8070 SB glass-ceramic. In addition, the fracture toughness of several other glasses was measured for comparison: soda-lime silicate, S8061 sealing glass, and a barium-strontium (Ba-doped) glass. With the exception of the as-molded 2164 glass, the test specimens were prepared by diamond grinding in conformance with ASTM C1161 (Ref. 3). For the 2164 glass specimens for crack growth testing, the tensile surface was preserved in the as-molded condition.

Experimental Procedure

The elastic modulus of 0120, 2164 and S8061 were determined at 20 °C by impulse excitation of vibration in accordance with ASTM C 1259 (Ref. 4). The mean and standard deviation of 0120 and S8061 were 73.3 ± 1.6 and 65.9 ± 0.1 respectively. The elastic modulus of 2164 in the as-molded and ground conditions was 62.0 ± 1.2 and 63.8 ± 0.5 GPa respectively.

Fracture strength as a function of stress rate was measured at 20 °C by using four point flexure of ASTM C1161 (Ref. 3) size B specimens (3×4 mm cross section loaded between 20 and 40 mm spans) at rates ranging from 10^{-3} to 10^{3} MPa/s in relative humidity ranging from ~2 to 95 percent. Humidity was controlled by testing in an enclosure connected to dry and moist air sources that were activated as needed by an electronic controller. Typically, six stress rates were applied with at least five specimens per rate. For the purposes of parameter analysis, the inert strength (i.e. the strength in the absence of a corrosive environment) was determined by testing at low RH (<2 percent) with a stress rate greater than or equal to 1000 MPa/s. This resulted in failure in a fraction of a second. To compare small, uniform precracks and cracks from natural abrasions, Ba-doped glass specimens were subjected to a 10N Vickers indentation load or abrasion via 150 grit abrasive paper.

Fracture toughness was measured by using chevron-notch flexure specimens (Ref. 5) in laboratory ambient (~30 percent RH) air or dry nitrogen. Test specimen stability was monitored via a strain gage placed on the compressive face of the specimen (Ref. 6).

Data Analysis

The power law formulation:

$$v = \frac{da}{dt} = AK_I^n = A^*\left[\frac{K_I}{K_{IC}}\right]^n \tag{1}$$

[1]Certain commercial materials are identified in order to adequately specify the experimental procedure and results. Such identification does not imply any endorsement.

was applied in the data analysis, where *v, a,* and *t* are crack velocity, crack size, and time, respectively. Constants *A* and *n* are the material/environment dependent SCG (slow crack growth) parameters, and K_I and K_{IC} are, respectively, the Mode *I* stress intensity factor and the critical stress intensity factor or fracture toughness of the material. For constant stress rate testing based on the power law formulation, the fracture strength, σ_f, is expressed as a function of stress rate as (Ref. 7)

$$\sigma_f = \left[B(n+1)\sigma_i^{n-2}\dot{\sigma}\right]^{1/n+1} \tag{2}$$

where $\dot{\sigma}$ is the applied stress rate, σ_i is the inert strength, and *B* is a parameter associated with *A, n*, fracture toughness, crack geometry and loading configuration (see Eq. (13)). The SCG parameter *n* can be determined from a plot of log σ_f as a function of log $\dot{\sigma}$ with Equation (2) written as

$$\log \sigma_f = \frac{1}{n+1}\log \dot{\sigma} + \log D \tag{3}$$

where

$$\log D = \frac{1}{n+1}\log\left[B(n+1)\sigma_i^{n-2}\right] \tag{4}$$

Once the slope α and intercept β are estimated by linear regression of Equation (3), the parameters *n*, *D*, *B* and *A*, and their standard deviation SD_n, etc., are estimated from (Ref. 8)

$$n = \frac{1}{\alpha} - 1 \tag{5}$$

$$SD_n \approx \frac{SD_\alpha}{\alpha^2} \tag{6}$$

$$D = 10^\beta \tag{7}$$

$$SD_D \approx 2.3026\left(SD_\beta\right)\left(10^\beta\right) \tag{8}$$

$$B = \frac{\alpha\left(10^{\beta/\alpha}\right)}{\sigma_i^{\left(\frac{1}{\alpha}-3\right)}} \tag{9}$$

$$SD_{\ln B} \approx \frac{1}{\alpha}\sqrt{Q^2\frac{SD_\alpha^2}{\alpha^2} + (\ln 10)^2 SD_{\hat{\beta}}^2 + (1-3\alpha)^2 SD_{\ln\sigma_i}^2 + 2Q\ln 10\frac{Cov(\alpha,\beta)}{\alpha}} \tag{10}$$

$$A^* = \frac{2K_{Ic}^2\sigma_i^{\left(\frac{1}{\alpha}-3\right)}}{10^{\beta/\alpha}(1-3\alpha)Y^2} = \frac{2K_{Ic}^2}{B(n-2)Y^2} \tag{11}$$

$$SD_{\ln A^*} \approx \frac{1}{\alpha}\sqrt{\begin{array}{l} 4\alpha^2 \dfrac{SD_{K_{Ic}}^2}{K_{Ic}^2} + \left(Q - \dfrac{\alpha}{1-3\alpha}\right)^2 \dfrac{SD_{\alpha}^2}{\alpha^2} + (\ln 10)^2 SD_{\beta}^2 \\ + (1-3\alpha)^2 SD_{\ln\sigma_i}^2 + 2\ln 10\left(Q - \dfrac{\alpha}{1-3\alpha}\right)\dfrac{Cov(\alpha,\beta)}{\alpha} \end{array}} \tag{12}$$

$$A = \frac{2K_{Ic}^{\left(3-\frac{1}{\alpha}\right)}\sigma_i^{\left(\frac{1}{\alpha}-3\right)}}{10^{\beta/\alpha}(1-3\alpha)Y^2} = \frac{2K_{Ic}^{2-n}}{B(n-2)Y^2} \tag{13}$$

$$SD_{\ln A} \approx \frac{1}{\alpha}\sqrt{\begin{array}{l} (3\alpha-1)^2 \dfrac{SD_{K_{Ic}}^2}{K_{Ic}^2} + \left(Q - \dfrac{\alpha}{1-3\alpha} - \ln K_{Ic}\right)^2 \dfrac{SD_{\alpha}^2}{\alpha^2} + (\ln 10)^2 SD_{\beta}^2 \\ + (1-3\alpha)^2 SD_{\ln\sigma_i}^2 + 2\ln 10\left(Q - \dfrac{\alpha}{1-3\alpha} - \ln K_{Ic}\right)\dfrac{Cov(\alpha,\beta)}{\alpha} \end{array}} \tag{14}$$

where $$Q = \alpha - \beta\ln 10 + \ln\sigma_i$$

and $$Cov(\alpha,\beta) = -SD_{\alpha}^2\left(\overline{\log\dot{\sigma}}\right) \tag{15}$$

where $\overline{\log\dot{\sigma}}$ is the mean of the logs of the applied stressing rates, Y is the geometry correction factor for the stress intensity factor, and the standard deviation associated with the inert strength ($SD_{ln\sigma i}$) is calculated in logarithmic space. Probability limits on the parameters B and A can be calculated from:

$$\underset{\text{Lower}}{B_{\text{Upper}}} = EXP\left[\ln B \pm t\left(SD_{\ln B}\right)\right] \quad \text{and} \quad \underset{\text{Lower}}{A_{\text{Upper}}} = EXP\left[\ln A \pm t\left(SD_{\ln A}\right)\right] \tag{16}$$

by using Student's t distribution for the DOF (degrees-of-freedom) and probability level desired. If the degrees-of-freedom (DOF) is greater than ~40, then

$$\underset{\text{Lower}}{B_{\text{Upper}}} = EXP\left[\ln B \pm \ell\left(SD_{\ln B}\right)\right] \quad \text{and} \quad \underset{\text{Lower}}{A_{\text{Upper}}} = EXP\left[\ln A \pm \ell\left(SD_{\ln A}\right)\right] \tag{17}$$

where ℓ is the number of standard deviations corresponding to the probability level desired. The DOF, ϕ, is given by

$$\begin{aligned} \frac{\left(SD_{\ln B}^2\right)^2}{\phi_{\ln B}} = \frac{1}{\phi_{\ln\sigma_i}}\left[\frac{(1-3\alpha)^2}{\alpha^2} SD_{\ln\sigma_i}^2\right]^2 + \\ \frac{1}{\phi_{\alpha\beta}}\left[Q^2\frac{SD_{\alpha}^2}{\alpha^4} + (\ln 10)^2\frac{SD_{\beta}^2}{\alpha^2} + 2Q\ln 10\frac{Cov(\alpha,\beta)}{\alpha^3}\right]^2 \end{aligned} \tag{18}$$

and

$$\frac{\left(SD^2_{\ln A}\right)^2}{\phi_{\ln A}} = \frac{1}{\phi_{\ln K_{Ic}}}\left(4SD^2_{\ln K_{Ic}}\right)^2 + \frac{1}{\phi_{\ln \sigma_i}}\left[\frac{(1-3\alpha)^2}{\alpha^2} SD^2_{\ln \sigma_i}\right]^2 + \frac{1}{\phi_{\alpha\beta}}\left[\left(Q - \frac{\alpha}{1-3\alpha}\right)^2 \frac{SD^2_{\alpha}}{\alpha^4} + (\ln 10)^2 \frac{SD^2_{\beta}}{\alpha^2} + 2\ln 10\left(Q - \frac{\alpha}{1-3\alpha}\right)\frac{Cov(\alpha,\beta)}{\alpha^3}\right]^2 \quad (19)$$

where ϕ_{σ_i} is the DOF in inert strength (number of inert strength tests minus one) and $\phi_{\alpha\beta}$ is the DOF in regression (number of constant stress rate tests minus two).

Three approaches were used to estimate the slope and intercept of Equation (3): linear regression of (1) the individual data points; (2) the median values; and (3) the average values. In addition to the approaches described, the fits were performed over several stress rate ranges to determine the sensitivity to inclusion of large stress rates.

Results

Fracture Toughness

Examples of load versus backface strain curves for laboratory air and dry N_2 are shown in Figure 1 for the Electro-Glass 2164. Stable fracture was exhibited in both environments; however, less stability was exhibited in dry N_2. Fracture toughness of the glasses tested exhibited a narrow range in dry N_2 (0.67 to 0.80 MPa√m), as summarized in Table 1. The fracture toughness of the glasses is nominally 3/4 MPa√m. Testing in air (30 to 60 percent RH) reduced the measured fracture toughness significantly. The S8070 glass-ceramic exhibited more than twice the fracture toughness of the glasses.

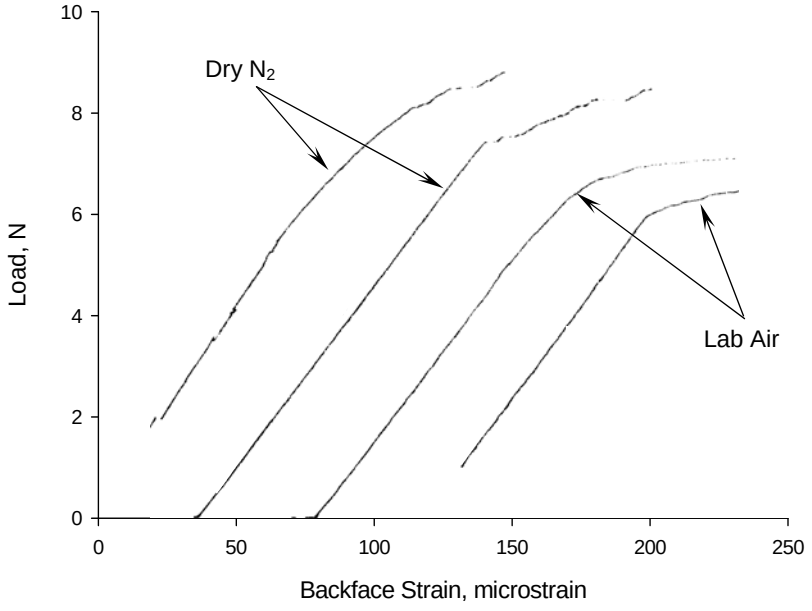

Figure 1.—Load as a function of backface strain for Electro-glass 2164 chevron-notched flexure specimens in dry nitrogen and laboratory air.

TABLE 1.—FRACTURE TOUGHNESS (MPa√M) OF GLASSES

Material	Environment	
	Air (%RH/°F)	Dry N_2
0120	0.50 ± 0.02 (34/76)	0.67 ± 0.02
2164	0.61 ± 0.05 (32/73)	0.74 ± 0.03
S8061	0.64 ± 0.01 (23/73)	0.72 ± 0.02
S8070	1.57 ± 0.03 (60/73)	1.90 ± 0.03
8330	0.61 ± 0.04 (60/73)	0.72 ± 0.04
Soda lime silicate	0.75 ± 0.04 (35/73)	0.80 ± 0.01
Ba-doped	0.72 ± 0.002 (23/73)	0.76 ± 0.01

Inert and Time-Dependant Strength

The fracture strength as a function of stress rate is plotted in Figures 2 through 5. The large degree of scatter, particularly at low RH, is indicative of the difficulty in characterizing and designing glasses and dense optical materials with strength measurements of the inherent flaw population: random and spurious damage make the distribution ever changing and difficult to characterize, regardless of Weibull statistics. In this testing, the effect of scatter on slow crack growth was mitigated partially by the large range of stress rates used (>four orders of magnitude). All the materials, except the S8070 SB glass-ceramic, exhibit a strength increase from ~50 MPa in 95 percent RH to ~150 MPa in 2 percent RH as the stress rate is increased from 0.001 MPa/s to 1000 MPa/s, implying a similar combination of flaw size distribution and fracture toughness. As the fracture toughness values are similar (Table 1), the implication is a similar flaw size distribution.

The slow crack growth parameters as estimated from Equations (5) to (17) are summarized in Table 2.

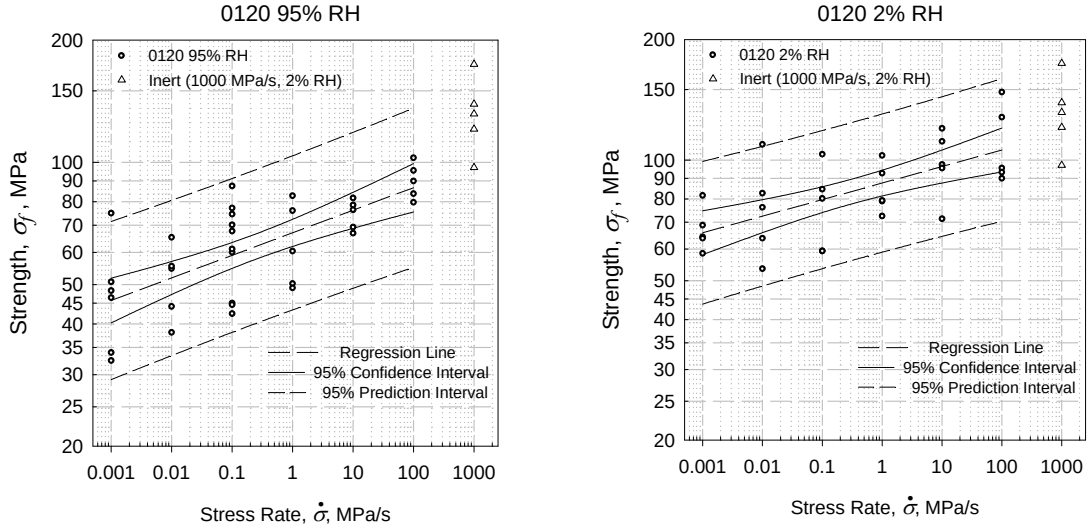

Figure 2.—Strength of 0120 glass in 2 and 95 percent relative humidity.

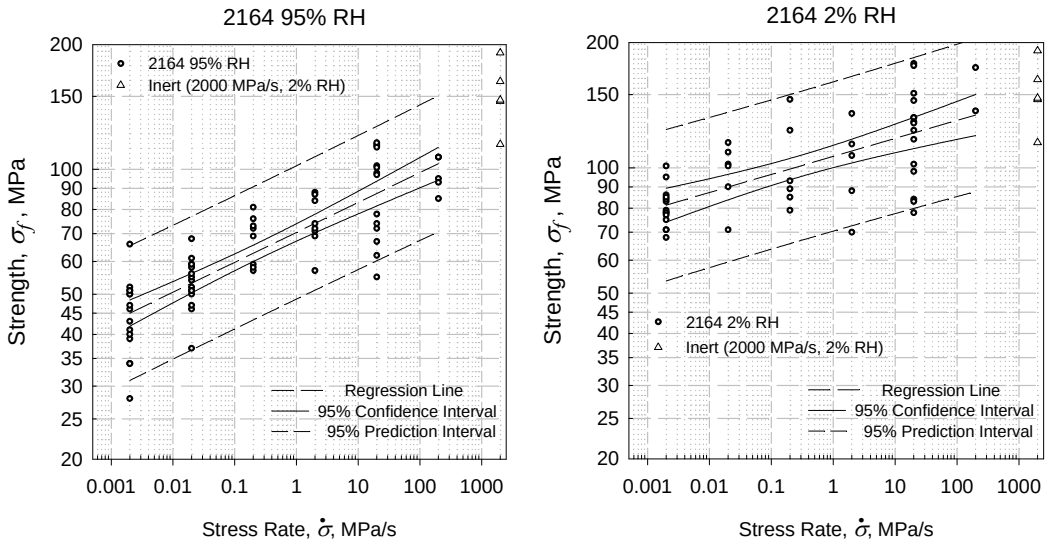

Figure 3.—Strength of 2164 glass in 2 and 95 percent relative humidity.

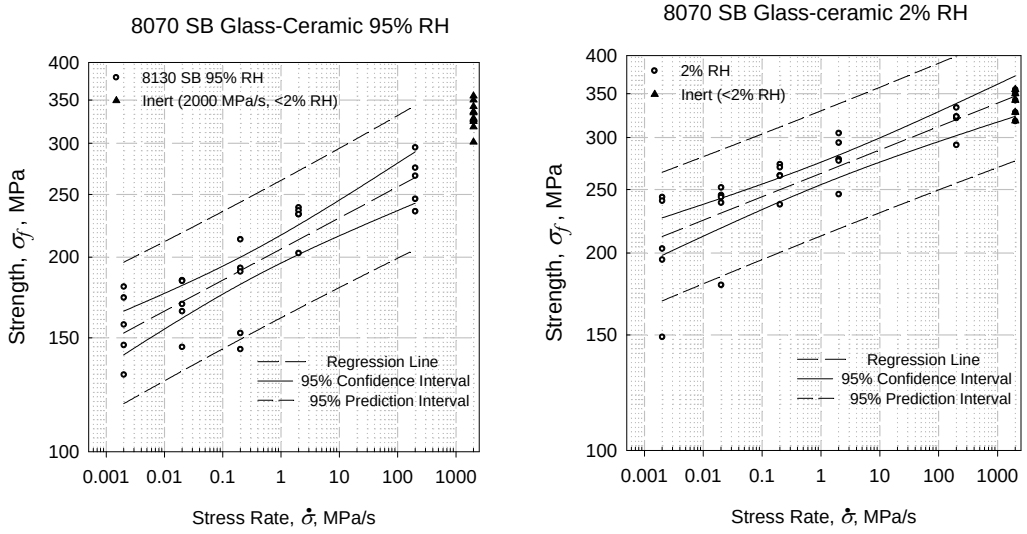

Figure 4.—Strength of S8070 SB glass-ceramic in 2 and 95 percent relative humidity.

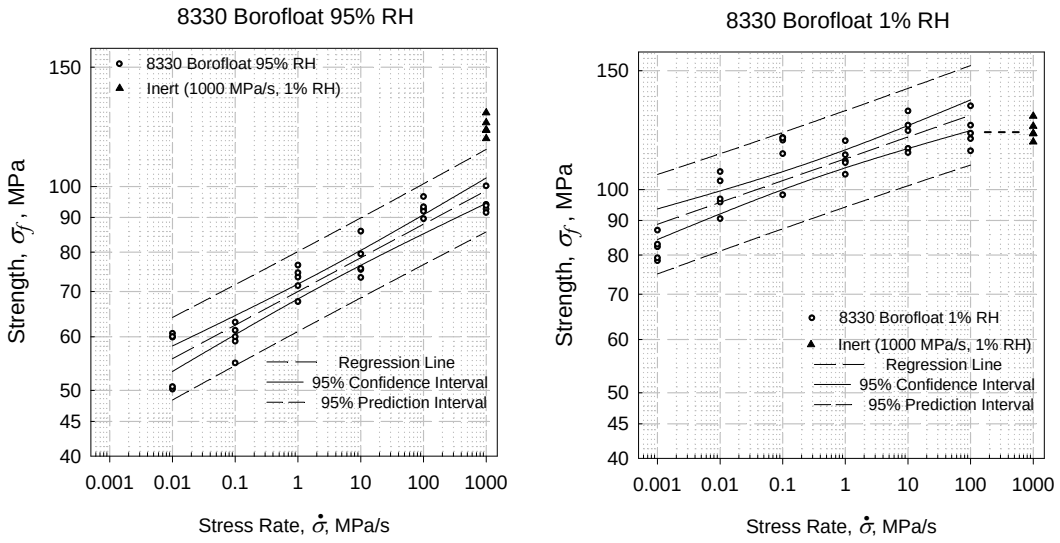

Figure 5.—Strength of 8330 borosilicate glass in 1 and 95 percent relative humidity.

TABLE 2.—SUMMARY OF SLOW CRACK GROWTH (SCG) PARAMETERS FOR GLASSES

Regression of Individual Points	n	B $MPa^2 \cdot s$	$B_{-95\%}$	A $m/s\ (MPa\sqrt{m})^{-n}$	$A_{+95\%}$	Number Tested
0120, 95% RH	17.0 ± 3.1	0.6	1.8×10^{-4}	$2.4\times10^{+1}$	$3.2\times10^{+5}$	36
0120, 2% RH	23.2 ± 5.3	4.3	1.0×10^{-4}	$2.8\times10^{+1}$	$1.2\times10^{+7}$	30
2164, 95% RH	12.9 ± 1.1	5.7	.06	2.3×10^{-1}	$3.4\times10^{+1}$	65
2164, 2% RH	22.1 ± 3.9	39	.01	3.0×10^{-1}	$4.4\times10^{+3}$	48
S8070, 95% RH	19.8 ± 2.6	60	1.6	4.9×10^{-9}	3.9×10^{-8}	25
S8070, 2% RH	25.0 ± 3.9	3,079	93	2.6×10^{-12}	1.2×10^{-10}	25
8330, 95% RH	17.1 ± 1.3	4.8	0.7	5.6×10^{-1}	$1.0\times10^{+1}$	25
8330, 3% RH	24.5 ± 3.9	19	0.4	8.0×10^{-1}	$3.1\times10^{+2}$	30
8330, 1% RH	30.0 ± 3.6	2,855	266	2.1×10^{-2}	$2.3\times10^{+0}$	30

Discussion

Effects of Humidity

Table 2 demonstrates that lower test humidity systematically results in higher estimates of n and B, regardless of the type of glass tested, implying that controlling or eliminating moisture via coatings, etc. will improve component life. The variances are also somewhat larger for dry conditions because the shallower slope is more difficult to characterize for the same stress-rate range. The parameters are also very sensitive to small changes in humidity at low humidity: the value of B changes by a factor of >100 for a change of 3 to 1 percent RH whereas a change from 95 to 3 percent RH results in a factor of <10 change.

Effect of Fit Method and Range

The effects of fit range and method on the estimated parameters can be seen in Tables 3 and 4: the fitting methods produce similar results for a data set; and the inclusion of the high stress rate data (1000 MPa/s) substantially alters the results at low humidity by increasing the estimated n. The lack of an effect of fit method implies either few outliers or sufficient data to mitigate the influence of outliers. The effect of fit range can be mitigated by using crack growth data only from lower stress rates (< ~200 MPa/s)

(Ref. 9), and independently measuring inert strength with ~0 percent RH. This avoids combining the different regions of the slow crack curve when estimating parameters.

TABLE 3.—COMPARISON OF FITTING RANGES AND METHODS FOR THE 8330 BOROSILICATE GLASS TESTED IN 95 PERCENT RH

Fit method	n	B $MPa^2 \cdot s$	A m/s $(MPa\sqrt{m})^{-n}$	Number Observed
All data (high rate included)				
Individual points	19.2 ± 1.3	1	3.7×10^{0}	30
Median values	21.6 ± 3.0	0.4	2.1×10^{1}	6
Average values	19.3 ± 2.0	1	3.9×10^{0}	6
< 1000 MPa/s (avoid inert region)				
Individual points	17.1 ± 1.3	5	5.6×10^{-1}	25
Median values	19.9 ± 3.6	1	4.5×10^{0}	5
Average values	17.2 ± 1.8	5	5.9×10^{-1}	5

TABLE 4.—COMPARISON OF FITTING RANGES AND METHODS FOR THE 8330 BOROSILICATE GLASS TESTED IN 1 PERCENT RH

Fit method	n	B $MPa^2 \cdot s$	A m/s $(MPa\sqrt{m})^{-n}$	Number Observed
All Data (high rate included)				
Individual points	36.8 ± 4.4	608	5.5×10^{-1}	35
Median values	38.2 ± 11.2	541	9.0×10^{-1}	7
Average values	36.8 ± 8.8	632	5.4×10^{-1}	7
< 1000 MPa/s (avoid inert region)				
Individual points	30.0 ± 3.6	2855	2.1×10^{-2}	30
Median values	30.4 ± 8.7	3032	2.2×10^{-2}	6
Average values	30.0 ± 7.0	2984	2.0×10^{-2}	6

Confidence Intervals

The 95 percent confidence intervals on B for the sealing glasses in Table 2 differ from the estimates by 1 to 3 orders of magnitude, even for data sets with 60 observations. The relatively large confidence intervals on some of the data sets imply that the use of inherent or natural flaws requires very large data sets. Improvements can also be made by maximizing the range of rates used, and by performing most of tests at the highest and lowest rates. However, as the test range is shifted to slower rates, the test time increases substantially. Monte Carlo estimates compared reasonably well with estimates from Equations (10) to (17), as shown on Table 5.

TABLE 5.—COMPARISON OF PROPAGATION-OF-ERRORS (POE) (EQS. (10) TO (17)) AND MONTE CARLO ESTIMATES

Relative Humidity (2164)	Method	B $MPa^2 \cdot s$	$B_{-95\%}$ $MPa^2 \cdot s$	A m/s $(MPa\sqrt{m})^{-n}$	$A_{+95\%}$ m/s $(MPa\sqrt{m})^{-n}$
95%	POE	5.7	0.06	0.230	34.1
	Monte Carlo	6.1	0.11	0.217	20.2
<2%	POE	39	0.009	0.298	4,361
	Monte Carlo	41	0.011	0.263	12,891

Crack Velocity

The crack velocity as a function of stress intensity based on the estimated parameters in Table 2 is shown in Figures 6 and 7. The S8070 glass-ceramic exhibited the least crack velocity whereas the 0120 and 2164 glasses exhibited the greatest velocities at any stress intensity. Application of common time-to-

failure equations (Ref. 7) indicate that the sustainable stress for the S8070 is doubled if the humidity is changed from 95 to 2 percent. As compared to soda-lime silicate float glass, the sealing glasses exhibit greater susceptibility to slow crack growth, as shown in Figure 6.

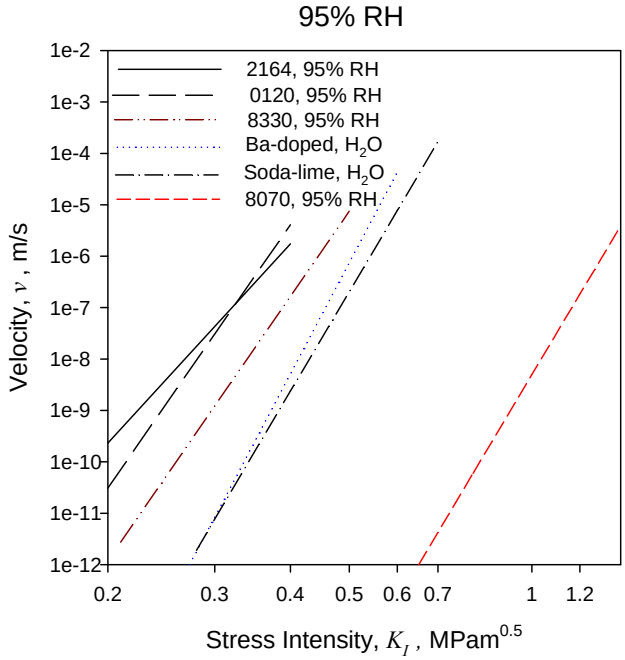

Figure 6.—Crack velocity for 95 percent relative humidity based on the parameters in Table 2.

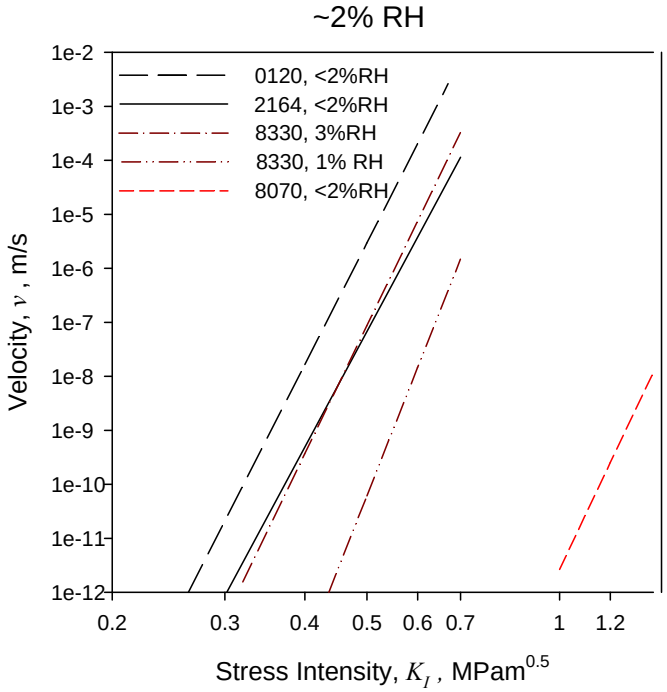

Figure 7.—Crack velocity for 1 to 3 percent relative humidity based on the parameters in Table 2.

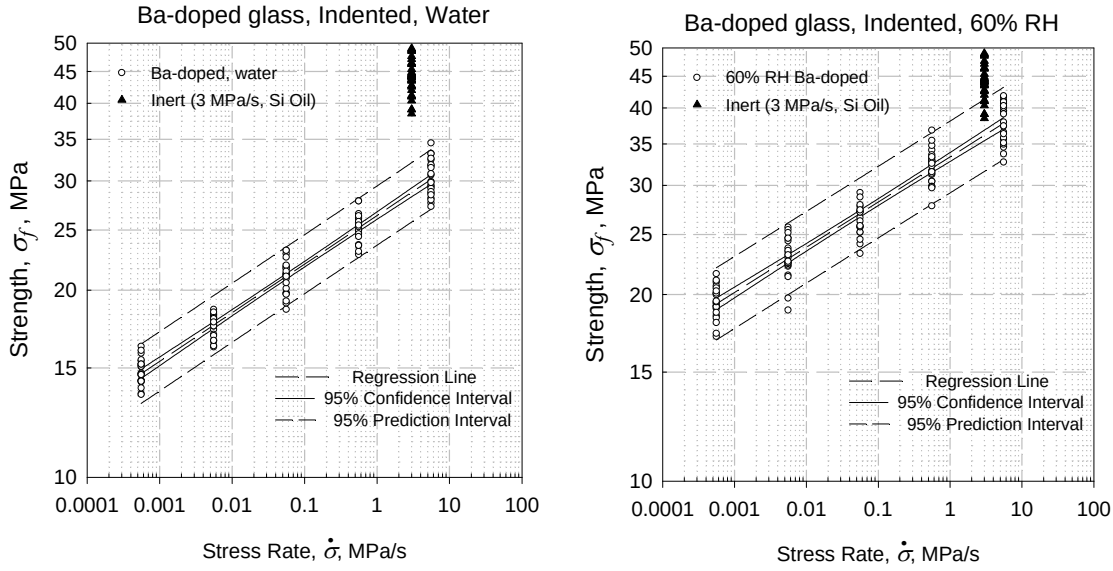

Figure 8.—Strength of Ba-doped glass in 60 percent RH air and distilled water.

Reduction of Scatter

Scatter in strength tests is reduced when the initial flaw population is made more uniform. This can be achieved by introducing a precrack, such as that formed when a brittle material is indented or scratched. In order to compare results from various flaw types and determine if scatter could be reliability reduced, a series of Ba-doped glass specimens were tested after either abrading with 150J grit alumina cloth or after precrecaking with a Vickers indenter at 10N. Abrasion left long, shallow surface cracks while indentation left deeper semi-elliptical cracks about the indentation. The abraded specimens were subjected to either uniaxial or biaxial flexure testing, while the indented specimens to uniaxial flexure. Environments of 60 percent RH air or distilled water were used. The inert strength was measured in silicone oil, and the fracture toughness was measured by using the chevron-notched beam (see Table 1) and the single-edged-precracked-beam (Ref. 5), which gave a slightly lower fracture toughness of 0.73 MPa√m. An example of fracture stress as a function of stress rate for abraded specimens subjected to biaxial flexure is shown in Figure 8. Because the precrecaking process results in residual stress about the crack, the correction factors of Fuller (Ref. 10) were used to estimate the parameters shown in Table 6:

$$n = 4n'/3 - 2/3 \text{ and } B = B'\left[\frac{3^{(n'-2)}}{(n-2)(4)^{(n-3)}}\frac{\Gamma(n)}{\Gamma(n')\Gamma(n-n')}\right] \quad \text{(point flaw)} \tag{20}$$

$$n = 2n' - 2 \quad \text{and } B = B'\left[\frac{1}{(n-2)(2)^{(n-3)}}\frac{\Gamma(n)}{\Gamma(n')\Gamma(n-n')}\right] \quad \text{(line flaw)} \tag{21}$$

where n' is the uncorrected value calculated by assuming Equation (5), n is the value corrected for residual stresses, and $\Gamma(z)$ is the gamma function of the argument z. The associated standard deviations can be derived from propagation of errors:

$$SD_n^{\text{point flaw}} \approx \frac{2SD_{n'}}{\sqrt{3}} \tag{22}$$

$$SD_n^{\text{line flaw}} \approx \sqrt{2}SD_{n'} \tag{23}$$

The most consistent parameter sets result by using the point-flaw correction for the indented specimens and the line-flaw correction for the abraded specimens, and stress intensity factor coefficients for ½ penny and long surface cracks respectively ($Y = 1.28$ for indented and $Y = 1.95$ for abraded). This results in relatively similar values of $n = \sim 23$ for abraded and $n = \sim 20$ for indented. Statistical comparison of the slopes (α's used to calculate n) by using the F statistic at 95 percent confidence indicate the slope estimates to be statistically different. Despite the differences in n, the values of B and A for a specific environment are very comparable for engineering purposes, as shown in Table 7.

TABLE 6.—COMPARISON OF PARAMETERS PRODUCED FROM INDENTED AND ABRADED SPECIMENS SUBJECTED TO UNIAXIAL AND BIAXIAL FLEXURE

Test Condition	n'	n Point flaw	n Line flaw	Number Tested
Abraded				
Uniaxial, Air	13.1 ± 0.4	17 ± 0.4	24 ± 0.5	115
" " , H_2O	12.2 ± 0.4	16 ± 0.4	22 ± 0.5	"
Biaxial, Air	12.7 ± 0.4	16 ± 0.4	23 ± 0.5	111
" " , H_2O	11.8 ± 0.3	15 ± 0.3	22 ± 0.4	112
Indented, uniaxial				
Air	15.5 ± 0.5	20 ± 0.6	29 ± 0.7	15
H_2O	14.8 ± 1.0	19 ± 1.1	28 ± 1.4	"
H_2O, Annealed	20 ± 1.1	-----	-----	25

TABLE 7.—PARAMETERS PRODUCED FROM INDENTED AND ABRADED SPECIMENS SUBJECTED TO UNIAXIAL AND BIAXIAL FLEXURE IN LAB AIR AND WATER

Test Condition	n	B $MPa^2 \cdot s$	A m/s $(MPa\sqrt{m})^{-n}$	Number Tested
Air				
Abraded, Uniaxial	24 ± 0.5	29	8.6×10^{-1}	115
Abraded, Biaxial	23 ± 0.5	37	5.7×10^{-1}	111
Indented, Uniaxial	20 ± 0.6	27	7.4×10^{-1}	15
Water				
Abraded, Uniaxial	22 ± 0.5	4.0	3.9×10^{-0}	115
Abraded, Biaxial	22 ± 0.4	2.7	4.7×10^{-0}	112
Indented, Uniaxial	19 ± 1.1	3.7	2.1×10^{-0}	15
Indented, Anneal	20 ± 1.1	8	1.1×10^{-0}	25

Parameters n and B generated in water are systematically smaller than those generated in lab air, in agreement with the sealing glass results. Biaxial and uniaxial testing produce very similar results. The effect of the difference in parameters on crack velocity between indented and abraded specimens can be seen in Figures 9 and 10. Overall, the velocities in water for the corrected parameters cluster better than those without correction.

Noteworthy are the small standard deviations of n produced by indentation despite the small number of tests (15 vs. 115). Also, they are less than ¼ of those for the sealing glasses. Probability limits on the parameter B' were estimated using Equations (10) and (16) and are given in Table 8. For the abraded specimens, about one order of magnitude exists between the estimated B, which is proportional to the time to failure, and $B_{-95\%}$. For the indented specimens, the difference is about ~1.5 orders, implying that a relatively small set of indented specimens can be used to reasonably estimate B.

TABLE 8.—PROBABILITY LIMITS ON CRACK GROWTH PARAMETER B' ESTIMATED FROM ABRADED AND INDENTED TEST SPECIMENS.

Test Condition	$B'_{\text{upper 95\%}}$	B'	$B'_{\text{lower 95\%}}$
Air			
Abraded, Uniaxial	921	92	9
Abraded, Biaxial	883	113	15
Indented, Uniaxial	1425	96	6
Water			
Abraded, Uniaxial	102	12	1
Abraded, Biaxial	53	8	1
Indented, Uniaxial	229	13	1
Indented, Annealed	62	14	3

The small but significant differences between n values from indentation and abrasion could be due to the abrasive not producing the residual stress field represented by the line flaw correction. This was investigated by testing specimens that were annealed at 520 °C for 2 hr after indentation. This removes the preexisting residual stresses associated with the indentation, and thereby eliminates the need for correction via Equation (20). As shown in Table 7 and Figure 10, good agreement is exhibited between the as-indented test data and annealed data, with less than an order of magnitude difference at any stress intensity. Similar results were found when soda-lime silicate was tested in as-indented and annealed conditions, as shown in Table 9. It should be noted that for the annealed test specimens, the strength at the largest stress rate is greater and more scattered than expected, as shown in Figure 11, implying that annealing blunts the crack tip. Evidently some time under load is required for a sharp crack to develop from the annealed crack, and again excessive stress rate must be avoided. The higher n values in Table 6 from Equation (21) imply that either the abraded specimens did not ideally represent line flaws or that Equation (21) slightly overestimates the necessary correction.

TABLE 9.—SUMMARY OF SLOW CRACK GROWTH PARAMETERS OF SODA-LIME SILICATE IN DISTILLED WATER

Test Condition	n	B $MPa^2 \cdot s$	A $m/s\ (MPa\sqrt{m})^{-n}$	Number Tested
Indented, corrected with Equation (20)	20.1 ± 0.9	5	7.5×10^{-1}	20
Indented then annealed	20.0 ± 2.0	18	2.1×10^{-1}	30

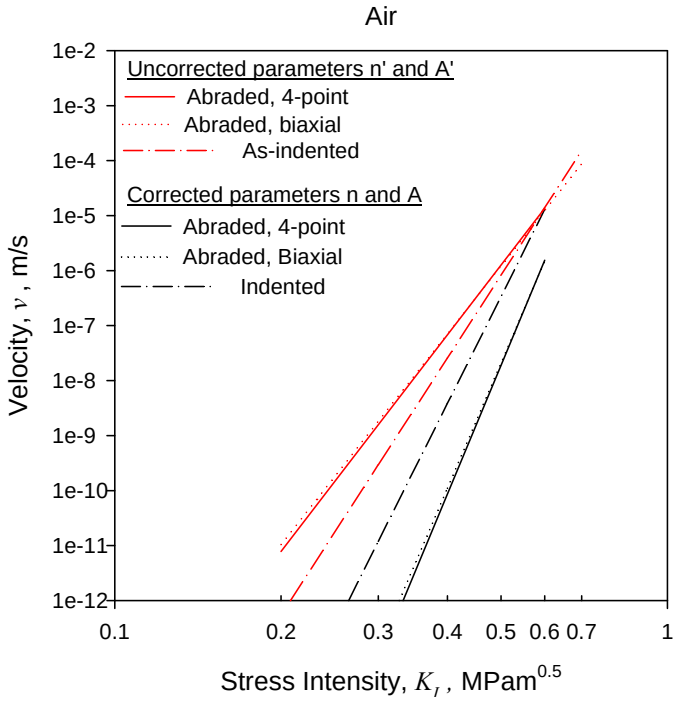

Figure 9.—Crack velocity of abraded and indented Ba-doped glass subjected to uniaxial and biaxial flexure in air.

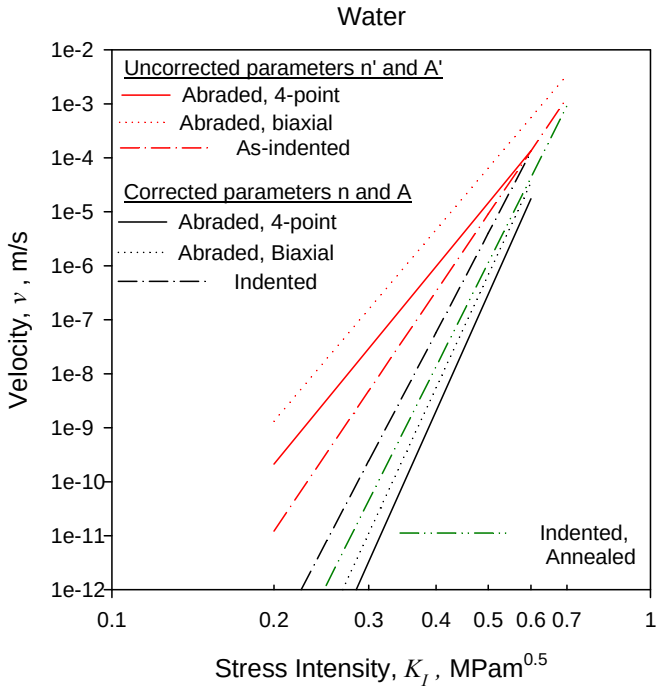

Figure 10.—Crack velocity of abraded and indented Ba-doped glass subjected to uniaxial and biaxial flexure in water.

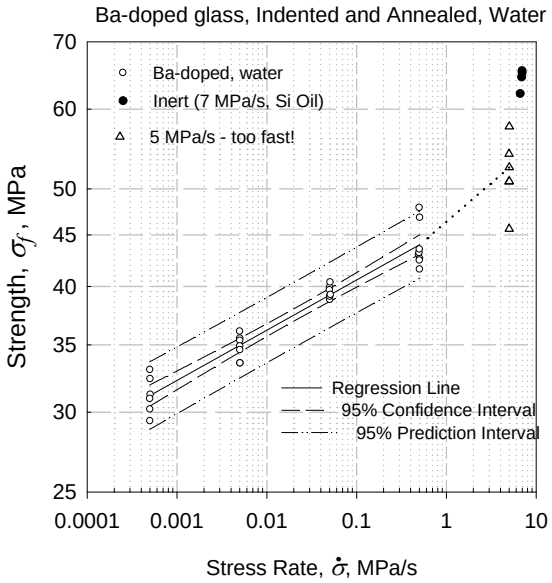

Figure 11.—Strength of Ba-doped glass as a function of stress rate in distilled water after indentation and annealing.

It should be noted that glass components may contain flaws with associated residual stresses, and the best parameters for design will depend on the exact circumstances. The most conservative approach is to use uncorrected parameters.

Conclusions

SCG parameters measured using constant stress rate testing in high humidity are systematically smaller (n and B) than those measured in low humidity. Velocities for dry environments are ~100x lower than for wet environments: keeping components dry should significantly extend the life. The crack velocity is very sensitive to small changes in RH at low RH: for the 8330 glass, a ~100x change in velocity results for an RH change of 1 to 3 percent and for 3 to 95 percent. S8070 SB glass-ceramic exhibits the lowest crack velocities of the sealing glasses tested, and reducing RH from 95 to 2 percent nearly doubles the sustainable stress.

The use of high stress-rate data increased estimates of n at low RH: Parameter fits to high stress rate data (e.g., >100 MPa/s) should be made with caution, especially for annealed material. Annealing of indentation cracks produce very similar parameters as as-indented specimens when a correction factor was applied. Indentation and abrasion flaws resulted in statistically similar values of B and A, however, estimates of n were significantly different by ~15 percent after correction for residual stresses. Biaxial and uniaxial stress states produced very similar crack growth parameters.

Monte Carlo simulations and propagation of errors solutions gave similar estimates of parameter variance. Future work should include measurement of the parameters with macro-crack test specimens for comparison.

References

1. NASGRO Fracture Mechanics and Fatigue Crack Growth Analysis Software, version 5.1, Southwest Research Institute, San Antonio, TX.
2. J.A. Salem “Mechanical Characterization of ZnSe Windows for use with the Flow Enclosure Accommodating Novel Investigations in Combustion of Solids (FEANICS) Module,” NASA/TM—2006-214100.

3. ASTM C 1161, “Standard Test Method for Flexural Strength of Advanced Ceramics at Ambient Temperature,” in *Annual Book of Standards*, Vol. 15.01, American Society for Testing and Materials, West Conshohocken, PA, 2004.
4. ASTM C 1259, “Standard Test Method for Dynamic Young’s Modulus, Shear Modulus, and Poisson’s Ratio for Advanced Ceramics by Impulse Excitation of Vibration,” in *Annual Book of Standards*, Vol. 15.01, American Society for Testing and Materials, West Conshohocken, PA, 2004.
5. ASTM C 1421-99 “Standard Test Method for the Determination of Fracture Toughness of Advanced Ceramics at Ambient Temperatures,” in Annual Book of ASTM Standards, V. 15.01, American Society for Testing and Materials, West Conshohocken, PA, 2000.
6. J.A. Salem and L. J. Ghosn, “Back-Face Strain as a Method For Monitoring Stable Crack Extension In Ceramics,” *Ceramic Engineering and Science Proceedings*, Vol. 19, No. 3, pp. 587-594, (1998).
7. J.E. Ritter, “Engineering Design and Fatigue Failure of Brittle Materials,” in *Fracture Mechanics of Ceramics*, Vol. 4, R. C. Bradt, D. P. H. Hasselman, and F. F. Lange, eds., Plenum Publishing Co., NY, 1978, pp. 661–686.
8. J.A. Salem and A.S. Weaver, “Estimation and Simulation of Slow Crack Growth Parameters from Constant Stress Rate Data,” pp. 579–596 in Fracture Mechanics of Ceramics: Active Materials, Nanoscale Materials, Composites, Glass, and Fundamentals, R.C. Bradt, D. Munz, M. Sakai and K. White, eds., Springer, 2005.
9. J.A. Salem and M.G. Jenkins, “The Effect of Stress Rate on Slow Crack Growth Parameters,” pp. 213–227 in *Fracture Resistance Testing of Monolithic and Composite Brittle Materials*, ASTM STP 1409, J.A. Salem, G.D. Quinn and M.G. Jenkins, eds., American Society for Testing and Materials, West Conshohocken, Pennsylvania (Jan. 2002).
10. E.R. Fuller, Jr., B.R. Lawn, R.F. Cook, “Theory of Fatigue for Brittle Flaws Originating from Residual Stress Concentrations,” J. Am. Ceram. Soc., 66 [5]: pp. 314–321, 1983.

REPORT DOCUMENTATION PAGE		Form Approved OMB No. 0704-0188

1. REPORT DATE *(DD-MM-YYYY)*	2. REPORT TYPE	3. DATES COVERED *(From - To)*
01-01-2010	Technical Memorandum	

4. TITLE AND SUBTITLE
Test Method Variability in Slow Crack Growth Properties of Sealing Glasses

5a. CONTRACT NUMBER

5b. GRANT NUMBER

5c. PROGRAM ELEMENT NUMBER

6. AUTHOR(S)
Salem, J., A.; Tandon, R.

5d. PROJECT NUMBER

5e. TASK NUMBER

5f. WORK UNIT NUMBER
WBS 441261.04.22.04.03

7. PERFORMING ORGANIZATION NAME(S) AND ADDRESS(ES)
National Aeronautics and Space Administration
John H. Glenn Research Center at Lewis Field
Cleveland, Ohio 44135-3191

8. PERFORMING ORGANIZATION REPORT NUMBER
E-16763-1

9. SPONSORING/MONITORING AGENCY NAME(S) AND ADDRESS(ES)
National Aeronautics and Space Administration
Washington, DC 20546-0001

10. SPONSORING/MONITOR'S ACRONYM(S)
NASA

11. SPONSORING/MONITORING REPORT NUMBER
NASA/TM-2010-216080

12. DISTRIBUTION/AVAILABILITY STATEMENT
Unclassified-Unlimited
Subject Category: 27
Available electronically at http://gltrs.grc.nasa.gov
This publication is available from the NASA Center for AeroSpace Information, 443-757-5802

13. SUPPLEMENTARY NOTES

14. ABSTRACT
The crack growth properties of several sealing glasses were measured by using constant stress rate testing in ~2 and 95 percent RH (relative humidity). Crack growth parameters measured in high humidity are systematically smaller (*n* and *B*) than those measured in low humidity, and crack velocities for dry environments are ~100x lower than for wet environments. The crack velocity is very sensitive to small changes in RH at low RH. Biaxial and uniaxial stress states produced similar parameters. Confidence intervals on crack growth parameters that were estimated from propagation of errors solutions were comparable to those from Monte Carlo simulation. Use of scratch-like and indentation flaws produced similar crack growth parameters when residual stresses were considered.

15. SUBJECT TERMS
Glass; Ceramics; Strength; Crack growth; Fracture toughness; Connectors

16. SECURITY CLASSIFICATION OF:			17. LIMITATION OF ABSTRACT	18. NUMBER OF PAGES	19a. NAME OF RESPONSIBLE PERSON
a. REPORT	b. ABSTRACT	c. THIS PAGE			STI Help Desk (email:help@sti.nasa.gov)
U	U	U	UU	22	19b. TELEPHONE NUMBER *(include area code)* 443-757-5802